HIGH ENERGY COULOMB SCATTERED ELECTRONS DETECTED IN AIR USED AS THE MAIN BEAM OVERLAP DIAGNOSTICS FOR TUNING THE RHIC ELECTRON LENSES*

P. Thieberger†, Z. Altinbas, C. Carlson, C. Chasman, M. Costanzo, C. Degen, K. A. Drees, W. Fischer, D. Gassner, X. Gu, K. Hamdi, J. Hock, A. Marusic, T. Miller, M. Minty, C. Montag, Y. Luo and A.I. Pikin, Brookhaven National Laboratory, Upton, NY 11973, USA
S.M. White, European Synchrotron Radiation Facility, BP 220, 38043 Grenoble Cedex, France

Abstract

A new type of electron-ion beam overlap monitor has been developed for the Relativistic Heavy Ion Collider (RHIC) electron lenses. Low energy electrons acquire high energies in small impact parameter Coulomb scattering collisions with relativistic ions. Such electrons can traverse thin vacuum windows and be conveniently detected in air. Counting rates are maximized to optimize beam overlap. Operational experience with the electron backscattering detectors during the 2015 p-p RHIC run will be presented. Other possible real-time non-invasive beam-diagnostic applications of high energy Coulomb-scattered electrons will be briefly discussed.

The present RHIC luminosity limitation for the collision of polarized protons, imposed by the beam-beam effect, is due to the non-linear lens effect of the macroscopic field of one bunch upon each proton in the opposite bunch. This "bad lens" causing tune-spread, emittance growth and gradual beam loss can be partially compensated with similar lenses of opposite polarity located at locations where the phase advances are integer numbers of π with respect to the pp interaction region. To accomplish this end, two electron lenses where installed in the RHIC tunnel and successfully used during the 2015 pp run [1]. To optimize the performance of such electron lenses, the electron and proton beams need to be accurately superimposed. Fig. 1 illustrates the effect of a 0.3 σ horizontal misalignment (100 μm for a 300 μm rms beam size) which is close to the maximum that can be tolerated.

To achieve such alignment with beam position monitors (BPMs) is challenging to say the least. The dc electron beam needs to be periodically interrupted which is not desirable for stable operation, and the signals thus generated are very different from the proton bunch signals, making electronic offsets practically unavoidable. It was realized at an early stage that a "luminosity" signal was required that could measure the degree of overlap directly.

At first, detecting bremsstrahlung from small impact parameter p-e collisions was considered, but it was soon realized that the electrons participating in such collisions would acquire high enough energies to allow these to be detected instead.

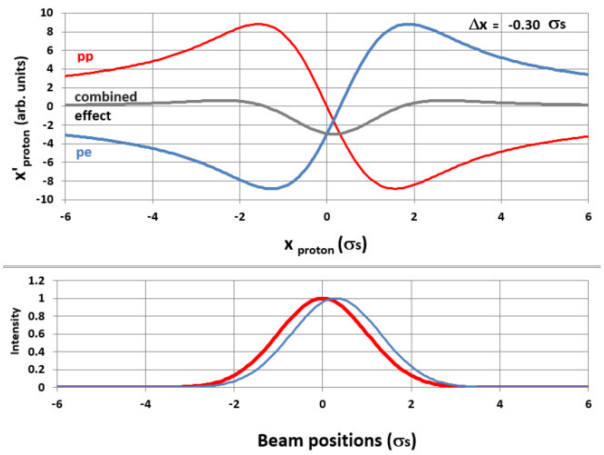

Figure 1: The radial kick from the colliding bunch (red) is partially compensated by an opposite kick from the electron lens (blue). The compensation is imperfect (grey) when the beams are misaligned. These curves are approximations obtained with simplified short beam-beam lens models for both the p-p and p-e interaction regions.

The theory of small-impact parameter collisions between charged particles has been well known since 1911 [2] when Ernest Rutherford discovered the atomic nucleus by studying the scattering of alpha and beta particles from stationary targets. Our targets, the protons, far from being stationary, are moving at relativistic velocities.

Fig. 2 illustrates the fact that a small angle deflection in the proton frame leads to a backscattered high energy (up to a several MeV) electron in the lab frame.

A simple theory (see [3] and references therein) was developed for estimating energies, angles and cross sections for producing such backscattered electrons. A coordinate transformation to the proton frame allows the application of the standard equations for Rutherford scattering. The inverse transformation of the results back to the lab frame yields electron energy and scattering cross sections such as the ones shown in Fig. 3.

* Work supported by Brookhaven Science Associates under Contract No. DE-AC02-98CH10886 with the U.S. Department of Energy.

Most of this material appears in an article by the same authors entitled "High energy Coulomb-scattered electrons for relativistic particle beam diagnostics", Phys. Rev. Accel. Beams 19, 041002 (2016)

† PT@BNL.GOV

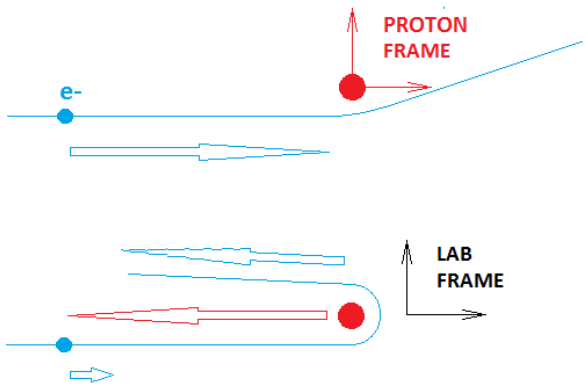

Figure 2: Schematic illustration of a small impact parameter collision of a low energy electron (~5 keV in our case) with a relativistic (e.g. 250 GeV) proton.

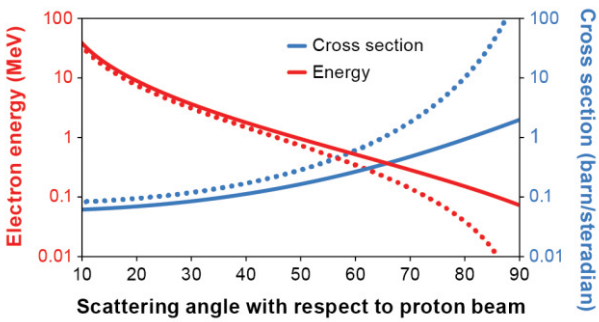

Figure 3: The solid lines show calculated energies and approximate scattering cross sections for 5 keV electrons backscattered by 250 GeV protons. The dotted lines correspond to the same quantities, but for 10 eV electrons as a qualitative indication of energetic electrons generated by the interaction of the beam with the residual gas.

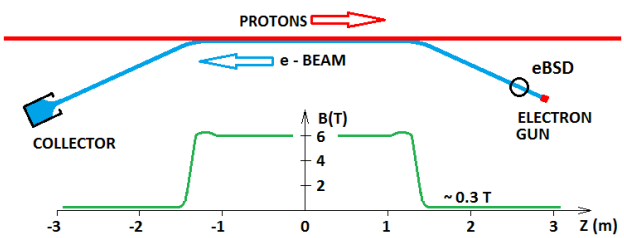

Figure 4: Schematic plan view of the electron beam trajectory in one of the e-lenses (top) and of the strength of the magnetic field guiding these electrons from the gun to the collector (bottom).

The geometry in which these backscattered electrons are generated and detected in an electron backscattering detector (eBSD) [3] is shown in the schematic plan view of one of the e-lenses depicted in Fig. 4

A side view of backscattered electrons spiralling towards de eBSD along the magnetic field lines is shown in Fig. 5. We see the spiralling trajectories of electrons as they exit the superconducting solenoids propagating towards the

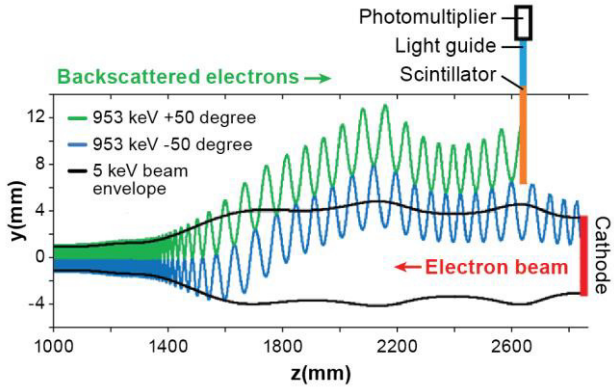

Figure 5: Simulated trajectories (blue and green curves) of two scattered electrons generated inside of the 6 T solenoid (see Fig. 4). Only the rightmost 200 mm of this 2400 mm long superconducting solenoid is included at the left.

electron gun. Some of these electrons exit the vacuum through a thin window and are detected in a plastic scintillator attached to a light guide connected to a photomultiplier tube (PMT). Due to the horizontal bend in the guiding field (see Fig. 4) the trajectories drift upward [4], thus facilitating the detection of the high energy scattered electrons by providing improved separation from the primary, low energy, electron beam. A not-to-scale schematic of the detector in its housing, including the magnetically shielded PMT is shown in Fig. 6. The $0.001 \times 6.35 \times 25.4$ mm^3, Ti-6Al-4V alloy vacuum window was tested up to three atmospheres differential pressure without bursting. The vertical position of the assembly can be varied by 25.4 mm, thus providing a counting rate adjustment.

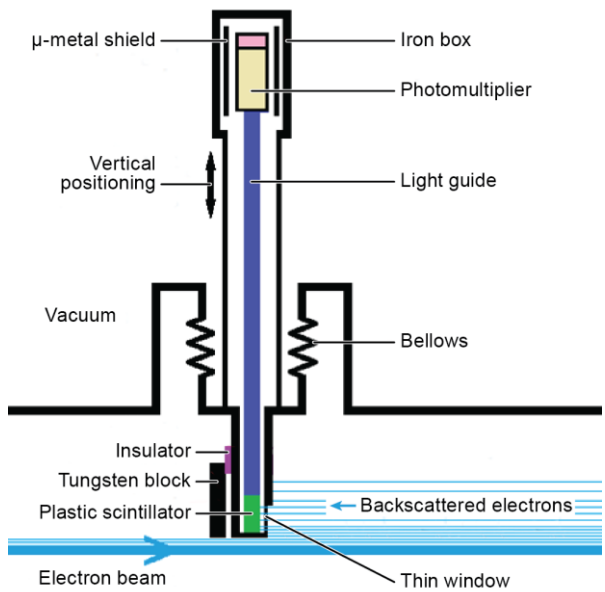

Figure 6: Not-to-scale schematic of the eBSD scintillation detector and its housing.

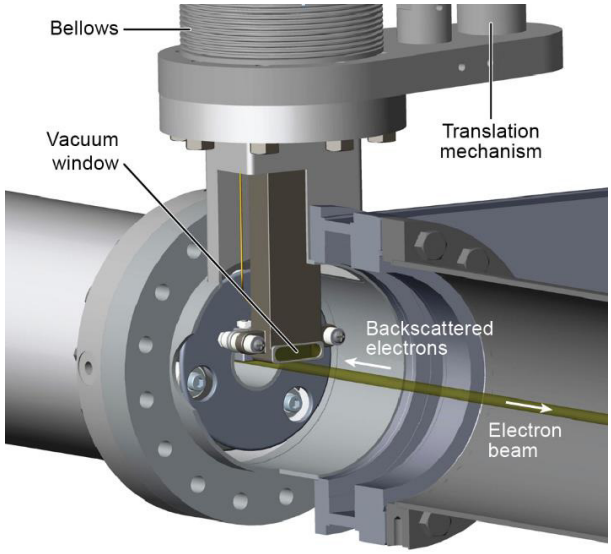

Figure 7: Cutaway drawing of the detector-housing and the vertical translation mechanism.

A tungsten block provides some protection against heating by the primary beam should the detector be accidentally lowered too much. A to-scale cutaway drawing is shown in Fig. 7 where the detector-housing is seen in its lowest position. Up to now, the detector was always used in the uppermost position to avoid excessively high counting rates.

Counting-rates as function ion electron beam displacements is shown in Fig. 8 for one of the first tests conducted with a 100 GeV/nucleon gold beam. The least-squares fitted Gaussian distributions are about 25% wider than expected. This small difference may be due to residual angular misalignments, to errors in estimating the widths of either beam or to beam instabilities.

Commissioning was continued with a ^{3}He beam in RHIC and beam separation scans were first performed manually (see Fig. 9) and then automated.

During the two-months long 2015 polarized proton RHIC run, the eBSD systems were fully functional and were utilized as the main alignment and monitoring tools to optimize electron and proton beam overlap in both e-lenses. The BPM systems were used to get the beams close so that some eBSD counting rates could be observed and from that point on, the counting rates were maximized to ensure alignment. Typical parameters for one of the storage periods are shown in Fig. 10. The overall luminosity gain due to e-lens compensation was estimated at 30% for this run [1]. Further luminosity increments would probably be impossible without this beam-beam effect compensation.

While background counts due to the residual gas were negligible during commissioning and use of the eBSD systems, this effect could be useful or else limiting in other possible beam diagnostic applications. Time-of-flight spectra of residual gas electrons accelerated by the proton beam were measured and can be seen in Fig. 11. Data were

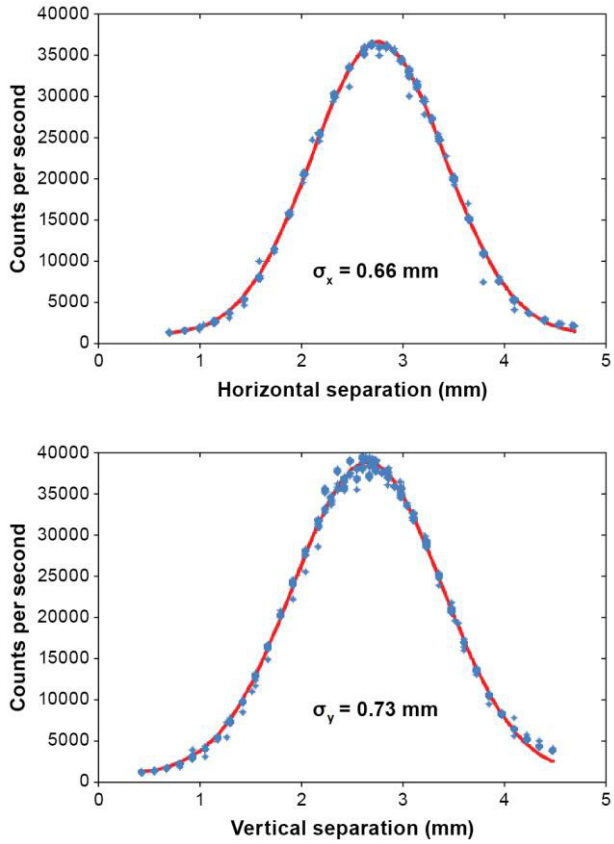

Figure 8: Horizontal and vertical beam separation scan obtained by steering the 5 keV electron beam with respect to the 100 GeV/nucleon gold beam.

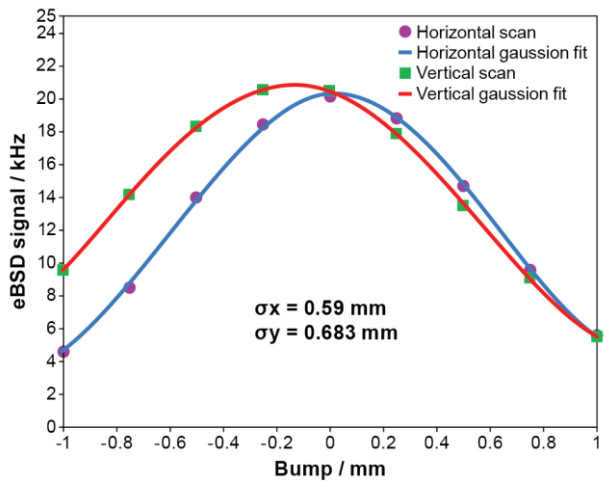

Figure 9: Manual beam separation scans obtained by stepwise steering the 3He beam with closed bumps utilizing part of the algorithm developed for the automated alignment optimization system based on the LISA program [5].

accumulated for 5 minutes due to the low counting rates. The top chart shows the RHIC 111-bunch pattern and

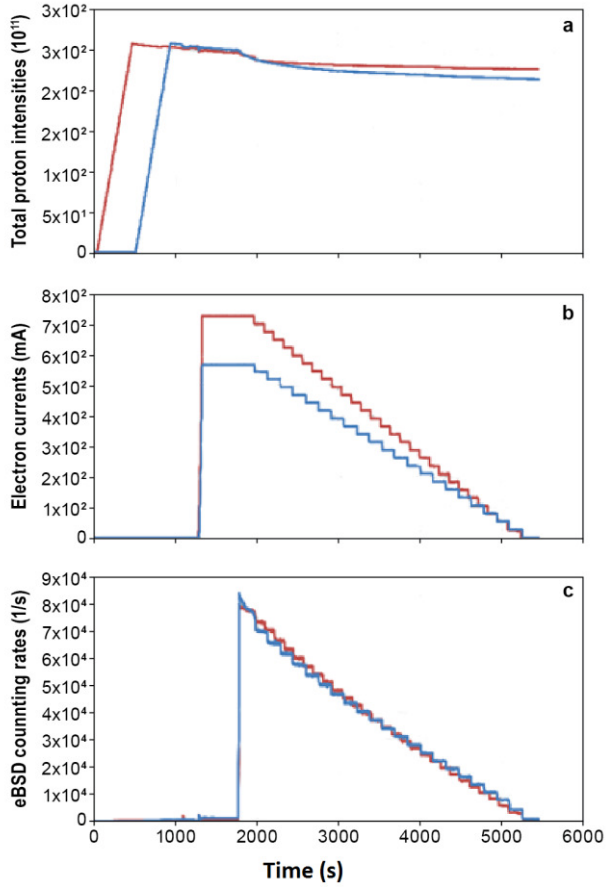

Figure 10: The total proton intensities (a), RHIC electron lens electron current intensities (b), and corresponding eBSD counting rates (c) are shown as a function of time. The electron beam intensities are reduced in steps to optimize the benefits of the RHIC electron lenses [1]. The two colors indicate the results from each of the two RHIC rings.

portions of the abort gaps preceding and following that pattern. The bottom chart is an expanded view of the last 10 bunches showing the asymmetric shape of the peaks due to the multitude of spiraling electron trajectories originating along the ~2.4m long interaction region.

The first example of another possible application of a system similar to the RHIC eBSDs is for alignment hollow electron beams. Here good alignment would be obtained by minimizing rather than maximizing the counting rate. Once good alignment is achieved, the system could be used as a halo monitor. Fig 12 shows three possible configurations. The bottom option eliminates the need of an annular cathode surrounding the ion beam (top option) which may be difficult to implement. It also avoids intersecting the electron and ion beams at a location that would produce background counts as would be the case for the middle configuration.

Electron beams that are not collinear with the relativistic ion beam will also generate energetic scattered electrons that can, in principle, be used for beam diagnostics. An example is schematically shown in Fig. 13. A ribbon shaped

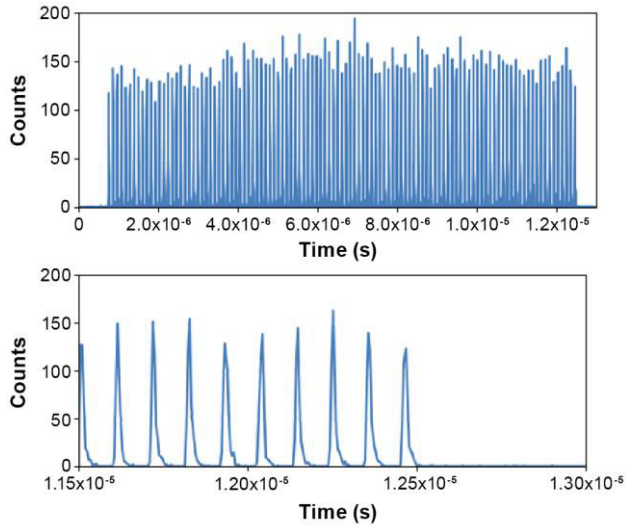

Figure 11: Time-of-flight spectra of electrons generated by the interaction of the relativistic proton beam with the residual gas. The bottom chart is an expanded view of the last 10 bunches to show the asymmetric shape of the peaks.

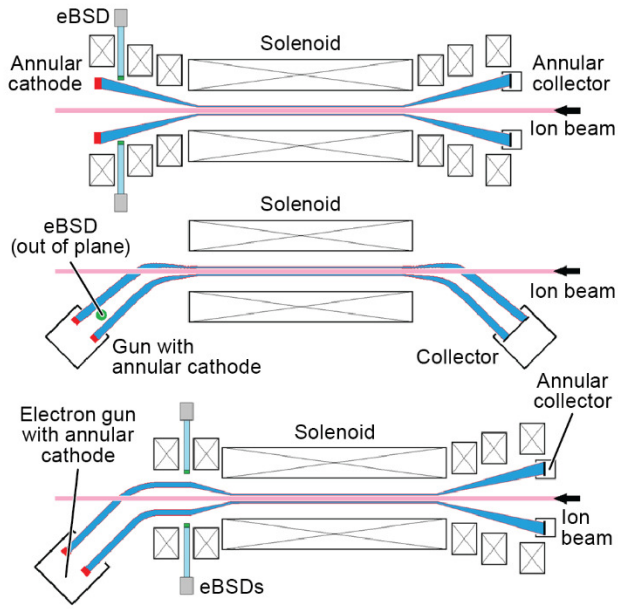

Figure 12: Three possible configurations for using eBSDs for halo monitoring and beam alignment of hollow electron beam systems.

electron beam propagates at a right angle to the ion beam guided by a weak magnetic field (2B) that affects the ion beam only slightly. This slight perturbation is compensated by the field B generated by the other two split solenoids.

The trajectories of the scattered electrons are bent in the field of the central split solenoid and some of them reach a scintillation detector through a vacuum window (not shown in the picture). Maximum intensity corresponds to optimal overlap. The beam profile can be explored by stepwise deflections of either the electron or the ion beam.

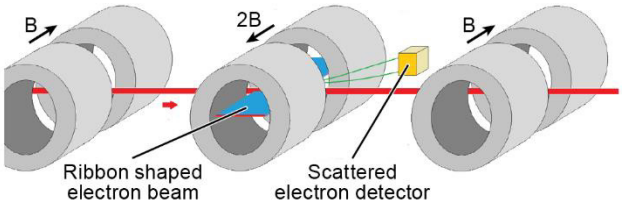

Figure 13: Schematic illustration of a Coulomb Scattering Electron Wire beam profile monitor

In contrast to conventional electron wire profile monitors [6, 7, 8], the profile is determined here by measuring the counting rates of the scattered electrons and not by detecting the deflection of the electron trajectories, largely suppressed here by the transverse magnetic field. Potential advantages are that the measured profiles are largely independent of the beam intensity and that profiles are obtained directly as deflection-dependent counting rates. For relatively long bunches, the arrival time of the scattered electrons can be used to measure the time structure and head-tail position differences for each bunch. Two such systems, one horizontal and one vertical, would provide a rather complete characterization of the bunch through non-destructive measurements.

Finally, as shown in Fig. 14, detecting high energy electrons scattered from residual gas molecules could in principle be used to develop a multiple beam position monitor [3] for the electrons beams in the proposed eRHIC machine [9] .

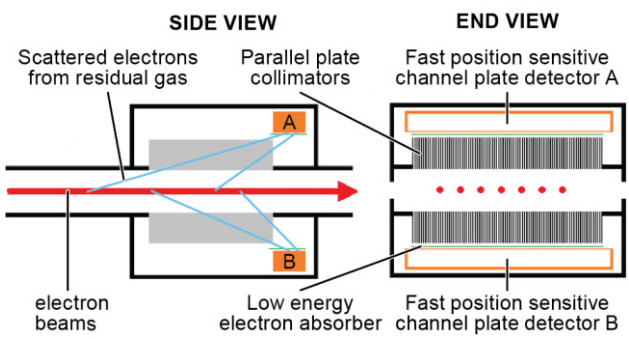

Figure 14: Concept of one of the possible approaches to detect several side-by-side orbits in one of the fixed-field alternating gradient (FFAG) arcs of the electron-ion collider, eRHIC [9], which will be proposed as a successor to RHIC. Fast, position-sensitive channel-plate detectors respond to energetic electrons collimated by parallel plate collimators.

In conclusion, high energy electrons produced in small impact parameter Coulomb interactions with relativistic ions are being used for beam alignment in the RHIC e-lenses. Based on this experience other such non-invasive beam diagnostic tools may be developed in the future.

REFERENCES

[1] W. Fischer, X. Gu, Z. Altinbas, M. Costanzo, J. Hock, C. Liu, Y. Luo, A. Marusic, R. Michnoff, T.A. Miller, A.I. Pikin, V. Schoefer, and P. Thieberger, Physical Review Letters, 115, 264801 (2015) .

[2] E. Rutherford, F.R.S., Philosophical Magazine, Series 6, vol. 21, May 1911, p. 669-688.

[3] "High energy Coulomb-scattered electrons for relativistic particle beam diagnostics", Phys. Rev. Accel. Beams 19, 041002 (2016). P. Thieberger, et. al. The present paper is an abridged version of this article by the same authors.

[4] J. D. Jackson, Classical Electrodynamics, Third Edition, John Wiley & Sons, Inc., 1999, page 590, equation 12.58.

[5] A. Drees and T. D'Ottavio, in *Proc. EPAC 2004*, Lucerne, Switzerland, p. 911.

[6] W. Blokland, A. Aleksandrov, S. Cousineau, D. Malyutin, S. Starostenko, in Proceedings of DIPAC09, Basel, Switzerland, paper TUOA03.

[7] W. Blokland and S. Cousineau, in *Proc. of 2011 Particle Accelerator Conference,* paper WEOCN2.

[8] V. Dudnikov and A. Aleksandrov, in *Proceedings IPAC2012*, New Orleans, Louisiana, U.S.A. paper MOPPD048.

[9] eRHIC design study: An Electron-Ion Collider at BNL. http://arxiv.org/abs/1409.1633